

## Phase-selection and metastable phase formation in highly undercooled eutectic $\text{Ni}_{78.6}\text{Si}_{21.4}$ alloys\*

LU Yiping<sup>1\*\*</sup>, YANG Gencang<sup>1</sup>, YANG Changlin<sup>1</sup>, WANG Haipeng<sup>2</sup> and ZHOU Yaohe<sup>1</sup>

(1. State Key Laboratory of Solidification Processing, Northwestern Polytechnical University, Xi'an 710072, China; 2. Department of Applied Physics, Northwestern Polytechnical University, Xi'an 710072, China)

Received May 10, 2005; revised June 28, 2005

**Abstract** A large undercooling (250 K) was achieved in eutectic  $\text{Ni}_{78.6}\text{Si}_{21.4}$  melt by the combination of molten-glass denucleation and cyclic superheating. The metastable phase formation process in the bulk undercooled eutectic  $\text{Ni}_{78.6}\text{Si}_{21.4}$  melts was investigated. With the increase of undercooling, different metastable phases form in eutectic  $\text{Ni}_{78.6}\text{Si}_{21.4}$  melts and part of these metastable phases can be kept at room temperature through slow post-solidification. Under large undercooling, the metastable phases  $\beta_2\text{-Ni}_3\text{Si}$ ,  $\text{Ni}_{31}\text{Si}_{12}$  and  $\text{Ni}_3\text{Si}_2$  were identified. Especially, the  $\text{Ni}_3\text{Si}_2$  phase was obtained in eutectic  $\text{Ni}_{78.6}\text{Si}_{21.4}$  alloy for the first time. Based on the principle of free energy minimum and transient nucleation theory, the solidification behavior of melts was analyzed with regard to the metastable phase formation when the melts were in highly undercooled state.

**Keywords:** undercooling, molten-glass, metastable phase, rapid solidification.

Ni-base alloys are widely applied in many industry fields, owing to their excellent properties. Eutectic alloy is extensively applied in all of the casting alloys. The excellent nature of the alloy is directly related to its composite phase. Therefore, phase selection in eutectic alloy is of importance in both theoretical investigation and practical application<sup>[1-3]</sup>. The phase selection process under rapid solidification conditions is not solely dependent on alloy composition but on process parameters, such as the cooling rate, temperature gradient and melt undercooling prior to solidification. Previously, rapid quenching methods were successfully applied to produce metastable solids from the liquid. Some metastable materials with new physical properties were discovered, which makes them suitable for new high performance materials in mechanical and electrical engineering. In order to develop a predictive capability for mode of metastable solidification, efforts are concentrated on the understanding, description and modeling of the physical mechanisms relevant to the formation of metastable phases. From the thermodynamic point of view, the undercooling is a necessary precondition for the solidification of metastable phases<sup>[4]</sup>. Nucleation in the undercooled melt selects the crystalline phase, stable or metastable phase before subsequent solidification completes<sup>[5]</sup>. Solidification of the highly undercooled

metallic alloy can lead to the formation of metastable solid phase. Since conventional rapid solidification process is hardly accessible to direct observation, it is difficult to reveal the solidification pathway. However, the high undercooling can not only achieve the rapid solidification of bulk alloy melts, but also monitor nucleation and growth in melts. The molten-glass denucleation method is an effective method for investigating the rapid solidification in highly undercooled alloy melts. In the present experimental conditions, the molten-glass denucleation and cyclic superheating and cooling are applied to remove the most potential nucleation agents from the melts, thus achieving high undercooling and even hyper-undercooling in bulk alloy melts. When  $\Delta T_{\text{hyp}} \geq \Delta H_m/C_p + (T_1 - T_0)$  ( $\Delta H_m$  is the latent of fusion,  $C_p$  is specific heat of liquid,  $T_1$  is the liquidus temperature,  $T_0$  is the temperature at which the congruent liquid/solid Gibbs energy is equal), solidification is completely proceeded at the temperature below  $T_0$  and the hyper-undercooled melts can implement bulk rapid solidification, so metastable phase formed during rapid solidification can be preserved at room temperature. With the development of rapid solidification, many different metastable phases have been detected in Nb-Al<sup>[6]</sup>, Ni-Nb<sup>[7]</sup>, Ni-B<sup>[8]</sup>, Fe-B<sup>[9]</sup>, Al-Co<sup>[10]</sup>, and Fe-Cr-Ni<sup>[11]</sup> alloys. At present, the existing theory of equi-

\* Supported by National Natural Science Foundation of China (Grant No. 50395103) and the Doctorate Foundation of Northwestern Polytechnical University

\*\* To whom correspondence should be addressed. E-mail: luyiping80818@hotmail.com

librium solidification cannot explain the protean non-equilibrium structure. Moreover, much difficulty exists to forecast, develop and control these metastable phases both in theory and in technology.

In this paper, the metastable phases  $\text{Ni}_{31}\text{Si}_{12}$ ,  $\text{Ni}_3\text{Si}_2$ , and  $\beta_2\text{-Ni}_3\text{Si}$  are obtained in highly undercooled eutectic  $\text{Ni}_{78.6}\text{Si}_{21.4}$  alloy. The formation of metastable phase is researched in highly undercooled eutectic alloy that is very important both in theory and application. The phase selection in the undercooled eutectic  $\text{Ni}_{78.6}\text{Si}_{21.4}$  alloy is theoretically analyzed based on the thermodynamic data.

## 1 Experiment

The experiment was performed in a high frequency induction facility. The master alloys of  $\text{Ni}_{78.6}\text{Si}_{21.4}$  were prepared with 99.99% pure Ni and 99.9999% pure Si *in situ* melting covered with  $\text{B}_2\text{O}_3$  glass in the high-purity silica crucible. The spherical sample weight was about 7 g. The glass denucleation agent was obtained by melting  $\text{B}_2\text{O}_3$  at 1373 K for 5 hours. A SCIT-II infrared pyrometer calibrated with a standard PtRh30-PtRh6 thermocouple was employed to record the cooling curves of the specimens which possess an absolute accuracy of  $\pm 5$  K. The particular process was first described by Wei et al.<sup>[12]</sup>. The alloy was cyclically superheated and cooled so that a high undercooling was obtained. At the predetermined undercooling, the nucleation was stimulated with a nickel needle at the top of the sample, and rapid solidification of the melt occurred toward the other end spontaneously.

After finishing the experiment, the samples were polished and etched with water solution of HF and  $\text{H}_2\text{O}_2$  to examine the microstructure. The microstructure was examined by a PMG3 Olympus optical microscope and JSM-6460 Scanning Electronic Microscope (SEM). The phase and composition was identified by a INCAX-sight energy-dispersive X-ray (EDS) spectroscope, chemical assay method and X-ray diffraction utilizing the Cu  $K\alpha$  line. The accuracy of the EDS measurements was within  $\pm 0.5\text{at}\%$ . Within the accuracy of the chemical assay, the overall compositions of the specimens did not change during a glass flux denucleation experiment.

## 2 Results and discussion

The Ni-Si binary alloy phase diagram is shown in Fig. 1. According to the Ni-Si phase diagram<sup>[13]</sup>, L

$\rightarrow \alpha\text{-Ni} + \beta_3\text{-Ni}_3\text{Si}$  phases are formed in eutectic reaction at the composition of  $\text{Ni}_{78.6}\text{Si}_{21.4}$  under equilibrium conditions. The primary phase  $\beta_3\text{-Ni}_3\text{Si}$  forming at high temperature goes through a polymorphic transformation and a eutectoid transformation during cooling, i. e. polymorphic transformation  $\beta_3\text{-Ni}_3\text{Si} \rightarrow \beta_2\text{-Ni}_3\text{Si}$  and eutectoid transformation  $\beta_3\text{-Ni}_3\text{Si} \rightarrow \beta_1\text{-Ni}_3\text{Si} + \gamma$  take place. The two solid-state transformations of the primary  $\beta_3\text{-Ni}_3\text{Si}$  phase cause only minor changes of the crystal structure and composition and therefore do not influence the resulting microstructure<sup>[14]</sup>.

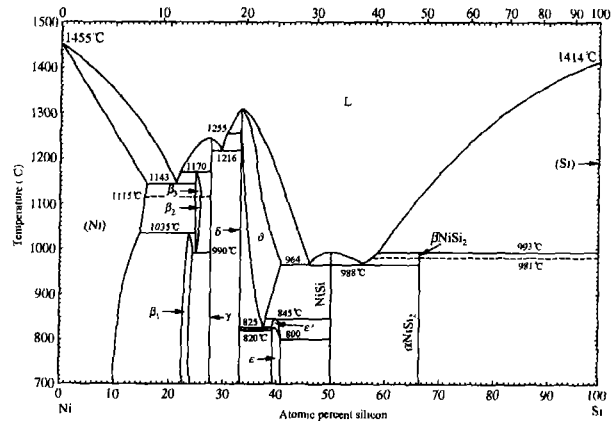


Fig. 1. Phase diagrams of binary Ni-Si.

### 2.1 Formation of metastable phase

The samples were initially superheated up to 200 K with respect to the eutectic temperature. In the experiments, a maximum undercooling of 250 K was achieved. The solidification starts by spontaneous nucleation if a certain undercooling level is achieved upon cooling. Alternatively, it was triggered at a controlled undercooling level, thus the desirable metastable phase can be obtained by controlling the undercooling. Metastable  $\beta_2\text{-Ni}_3\text{Si}$  phase is obtained at undercooling 72 K, and some unidentified particles are distributed in it (Fig. 2(a)). Metastable  $\beta_2\text{-Ni}_3\text{Si}$  phase presents non-planar morphology owing to large undercooling. From Fig. 2(b), it can be found that parts of  $\alpha\text{-Ni}$  dendrite remelt. Physically, this process is driven by surface tension and solute trapping in rapid solidification which changes the melting point of as-formed phases. In the undercooling regime of 0–180 K, The metastable  $\text{Ni}_{31}\text{Si}_{12}$  phase is derived.  $\beta_1\text{-Ni}_3\text{Si}$  phase can only be partially replaced by  $\text{Ni}_{31}\text{Si}_{12}$  and  $\text{Ni}_3\text{Si}_2$  phases because these metastable phases decompose on slow post-solidification, as shown in Fig. 2(b), (c), (d). The  $\text{Ni}_{31}\text{Si}_{12}$  phase displays irregular morphology. A small quantity of

Ni<sub>3</sub>Si<sub>2</sub> phase is obtained at undercooling 250 K, which presents dark and irregular morphology in Fig. 2(d). It can be seen that some bright particles appear in Fig. 2(d), which are metastable phases proved by EDS and X-ray diffraction. However, its precise atomic ratio still cannot be affirmed. These metastable phases are also confirmed by X-ray diffraction patterns in Fig. 3. However,

some metastable phases are still not identified due to the limitation of the analysis data. On the one hand, the metastable phase particles are very small for high undercooling, so the sizes of these metastable phases are less than the least size of EDS analyses. On the other hand, the standard card of X-ray diffraction is limited. Accordingly, these metastable phases cannot be also identified by X-ray diffraction.

### 2.2 Activation energy of crystal nucleation

In fact, metastable phase formation is determined by many factors. When phase transformation happens at lower temperature, the metastable phase and stable phase, which one will be precipitated? Usually, emergence of metastable phase can be explained by thermodynamics and dynamics. Nucleation work of a specific crystallographic phase is characterized by activation energy ( $\Delta G^*$ ) to form a nucleus of critical size in the undercooled melt. The nucleation barrier arises from the interfacial energy ( $\sigma_{sl}$ ) between the crystal nucleus and the undercooled melt. According to classical nucleation theory and the ne-gentropic model by Spaepen<sup>[15]</sup> for the estimation of  $\sigma_{sl}$ ,  $\Delta G^*$  is given by

$$\Delta G^* = \frac{16\pi\sigma_{sl}^3}{3\Delta G^2} f(\theta), \quad (1)$$

where

$$\sigma_{sl} = \alpha \frac{\Delta S_f}{N_A^{1/3} \cdot V_m^{2/3}} T. \quad (2)$$

Here,  $\theta$  is the wetting angle,  $f(\theta) = 0.25(2 + \cos\theta)(1 - \cos\theta)^2$ ,  $\Delta G$  is the Gibbs free energy difference per unit volume between the solid and the liquid phase,  $\Delta S_f$  is the entropy of fusion,  $N_A$  is the Avogadro's number,  $V_m$  is the molar volume,  $T$  is the temperature, and  $\alpha$  is a factor depending on the structure of crystal nucleus. The Gibbs free energy difference  $\Delta G = \Delta S_f \cdot \Delta T$  is often determined by using the linear approximation proposed by Turnbull<sup>[16]</sup>. Hence, the barrier for nucleation, i. e. the interfacial energy  $\sigma_{sl}$  depends on the structure of the crystal nucleus. The interfacial energy is often determined by measuring the maximum undercooling attainable for the melt<sup>[17]</sup>.

The activation energy of crystal nucleation of different phases is illustrated in Fig. 4. According to Fig. 4, the nucleation work decreases with the increase of undercooling, which indicates that the increase of undercooling is helpful to nucleate. The

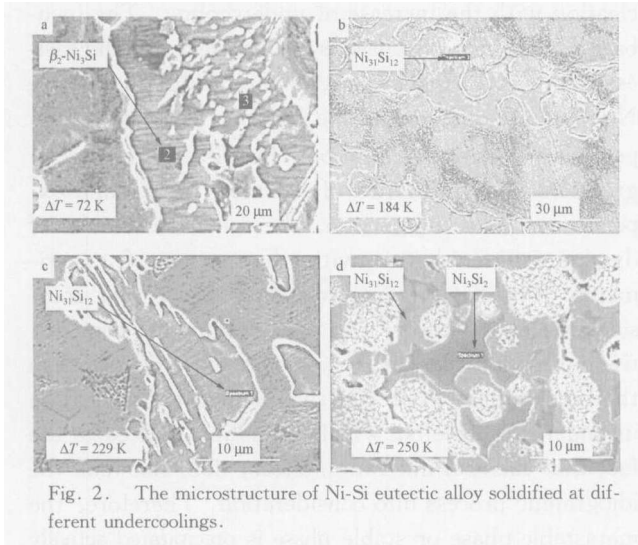


Fig. 2. The microstructure of Ni-Si eutectic alloy solidified at different undercoolings.

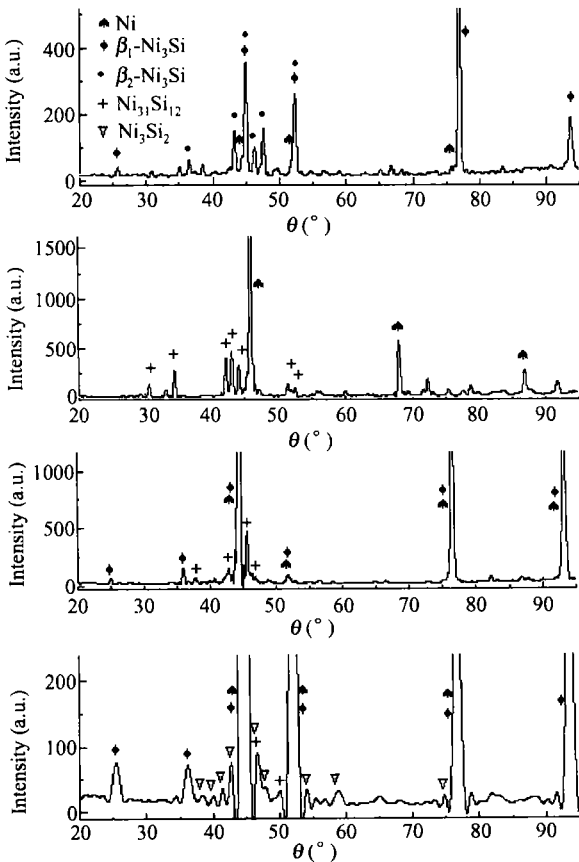


Fig. 3. X-ray diffraction spectrum of Ni-Si eutectic alloy solidified at different undercoolings.

competitive nucleation will happen between stable phase and metastable phase, or between metastable phase and metastable phase, under large undercooling. For example, competitive nucleations of  $\text{Ni}_3\text{Si}$  and  $\text{Ni}_{31}\text{Si}_{12}$  phases happen at far below their melting temperature. The nucleation work of the  $\alpha$ -Ni phase is the least one, so the  $\alpha$ -Ni phase is easier to nucleate than the other phases. The calculated result is well in agreement with the experiment result. However, thermodynamics can only give a rough estimate but not a precise forecast. The phase selection is determined not only by thermodynamic factors but also by kinetic factors.

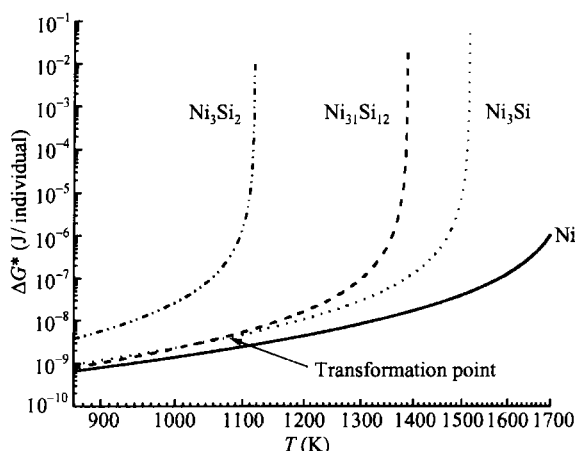


Fig. 4. Activation energy of nucleation of different phases with undercooling.

### 2.3 Kinetic analyses for metastable phase formation: transient nucleation

Apparently, the phase selection predicted by the calculated chemical Gibbs energy does not agree with the undercooling results. The value of Gibbs free energy is only for rough estimate. For the equilibrium metastable phase regions among different competing phases, further kinetic analysis is needed. Here, the transient nucleation theory proposed by Shao and Tsakiroopoulos<sup>[18]</sup> is adopted to analyze the nucleation behavior of various competing phases in the undercooled melts:

$$\tau = \frac{7.2Rf(\theta)}{1 - \cos\theta} \cdot \frac{a^4}{d_a^2 X_{L,eff}} \cdot \frac{T_t}{DS_m \Delta T_t^2}, \quad (3)$$

where  $T_t = T/T_m$ ,  $\Delta T_t = 1 - T_t$ ,  $S_m$  is the molar entropy of fusion,  $D$  is the diffusion coefficient and  $a$  is the atomic jump distance,  $d_a$  is the average atomic diameter of the solid phase,  $X_{L,eff}$  is the effective alloy concentration, and  $R$  is the gas constant. The temperature versus the  $\tau$  curves of eutectic

$\text{Ni}_{78.6}\text{Si}_{21.4}$  alloy is given in Fig. 5. The calculations are coupled with the data derived using the standard CALPHAD methods. The thermodynamic parameters of competing phases in Eqs. (1)–(3) are listed in Table 1. Two crossing points are marked in Fig. 5. It can be seen that metastable phase and stable phase, metastable phase and metastable phase compete in nucleation with the increase of undercooling. The incubation time of  $\alpha$ -Ni phase is the shortest and the easiest to nucleate. Under large undercooling, metastable  $\text{Ni}_3\text{Si}_2$  phase and metastable  $\text{Ni}_{31}\text{Si}_{12}$  phase will happen in competitive nucleation. This is also in good agreement with the result of thermodynamics and experiment. As a comparison, the calculated results of dynamics agree better with the results of experiments. The experimental results indicate that transient nucleation theory can well predict the competitive nucleation and the dynamics is more precise than thermodynamics to predict the competitive nucleation in undercooled melts, which is possibly related to the fact that classical nucleation theory does not take the idiographic process into consideration. Therefore, the metastable phase or stable phase is precipitated actually depending on the competitive nucleation process between them. Because the rapid solidification of high undercooling can lead to high solidification velocity, if

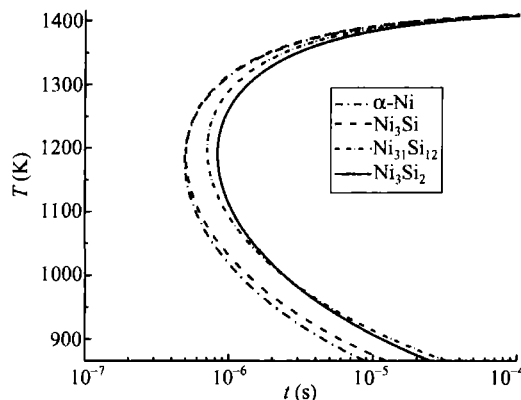


Fig. 5. The calculated  $T$  versus  $t$  for eutectic  $\text{Ni}_{78.6}\text{Si}_{21.4}$  alloy, showing a relation between the incubation times and undercooling of various phases ( $\alpha$ -Ni),  $\text{Ni}_3\text{Si}$ ,  $\text{Ni}_{31}\text{Si}_{12}$  and  $\text{Ni}_3\text{Si}_2$  nucleated from the undercooled melt.

Table 1. Thermodynamic parameters of competing phases<sup>a)</sup> [13, 19, 20, 21]

Phase	$X_{L,eff}$	$\Delta S$ ( $\text{J} \cdot \text{mol}^{-1} \cdot \text{K}^{-1}$ )	$\rho$ ( $\text{g} \cdot \text{cm}^{-3}$ )	$T_m$ (K)	$f(\theta)$	$W_m$ ( $\text{g} \cdot \text{mol}^{-1}$ )	$V_m$ ( $\text{cm}^3$ )
Ni	0.786	-10	8.9	1726	0.18	58.7	6.6
$\text{Ni}_3\text{Si}$	0.954	-7.6	7.6	1388	0.2	51	6.71
$\text{Ni}_{31}\text{Si}_{12}$	0.917	-8	7.4	1515	0.2	50.14	6.77
$\text{Ni}_3\text{Si}_2$	0.763	-5.0	6.7	1118	0.2	46.4	6.92

a)  $a = 32.4 \text{ nm}$ ;  $D = 8.07 \times 10^{-8} \text{ m}^2 \cdot \text{s}^{-1}$

the preferential nucleation of metastable phase can generally happen in undercooled melts, the formation of stable phase will be entirely restrained.

### 3 Conclusion

A large undercooling (250 K) has been achieved by the combination of molten-glass denucleation technology and cyclic superheating and cooling. Some metastable phases ( $\beta_2$ -Ni<sub>3</sub>Si, Ni<sub>31</sub>Si<sub>12</sub>, Ni<sub>3</sub>Si<sub>2</sub>) have been obtained in the highly undercooled eutectic Ni<sub>78.6</sub>Si<sub>21.4</sub> alloys. These metastable phases are verified by SEM, EDS and X-ray diffraction results. The solid-state transformation of the high temperature Ni<sub>3</sub>Si phases to the equilibrium  $\beta_1$ -Ni<sub>3</sub>Si phases in the undercooled samples can be partially suppressed. The thermodynamic and kinetic conditions of metastable phase formation are analyzed, which approves that metastable formation is affected by many factors. The metastable phase formation is controlled mainly by the nucleation competition. The transient nucleation theory is a good facility to predict the phase formation.

**Acknowledgement** We would like to thank Prof. Xiaoling Hu for her helpful discussion.

### References

- Zhou Y. H., Hu Z. Q. and Jie W. Q. Solidification Technique. Xi'an: China Machine Press, 1998. 36.
- Liu F., Yang G. C. and Kirchheim R. Overall effects of initial melt undercooling, solute segregation and grain boundary energy on the grain size of as-solidified Ni-based alloys. *J. Crystal Growth*, 2004, 264: 392—399.
- Wang H. P., Cao C. D. and Wei B. Thermophysical properties of a highly superheated and undercooled Ni-Si alloy melt. *Appl. Phys. Letts.*, 2004, 84: 4062—4064.
- Herlach D. M., Gao J., Holland-Moritz D. et al. Nucleation and phase-selection in undercooled melts. *Mater. Sci. Eng. A*, 2004, 375—377: 9—15.
- Herlach D. M. Non-equilibrium solidification of undercooled metallic melts. *Mater. Sci. Eng. R*, 1994, (12): 177—272.
- Löser W. R., Hermann R., Leonhardt M. et al. Metastable phase formation in undercooled near-eutectic Nb-Al alloys. *Mater. Sci. Eng. A*, 1997, 224: 53—60.
- Leonhardt M., Löser W. and Lindenkreuz G. H. Solidification kinetics and phase formation of undercooled eutectic Ni-Nb melts. *Acta Mater.*, 1999, 47(10): 2961—2968.
- Battezzati L., Antonione C. and Baricco M. Undercooling of Ni-B and Fe-B alloys and their metastable phase diagrams. *Journal of alloy and compounds*, 1997, 247: 164—171.
- Duhaj P. and Švec P. Formation of metastable phases from amorphous state. *Mater. Sci. Eng. (A)*, 1997, 226—228: 245—254.
- Schroers J., Holland-Moritz D., Herlach D. M. et al. Undercooling and solidification behaviour of a metastable decagonal quasicrystalline phase and crystalline phases in Al-Co. *Mater. Sci. Eng. A*, 1997, 226—228: 990—994.
- Koseki T. and Flemings M. C. Solidification of undercooled Fe-Cr-Ni Alloy: Part III. phase selection in chill casting. *Metall. Trans. A*, 1997, 28(11): 2385—2395.
- Wei B., Yang G. and Zhou Y. High undercooling and rapid solidification solidification of Ni-32.5% Sn eutectic alloy. *Acta Metall. Mater.*, 1991, 39: 1249—1258.
- Nash P. A. Phase diagrams of binary nickel alloy. *ASM International*, 1991, 229.
- Goetzinger R., Barth M. and Herlach D. M. Growth of lamellar eutectic dendrites in undercooled melts. *J. Appl. Phys.*, 1998, 84: 1643—1649.
- Spaepen F. A structural model for the solid-liquid interface in monatomic systems. *Acta Metall.*, 1975, 23(6): 729—743.
- Turnbull D. J. Formation of crystal nuclei in liquid metals. *J. Appl. Phys.*, 1950, 21: 1022—1028.
- Turnbull D. J. Kinetics of solidification of supercooled liquid mercury droplets. *J. Chem. Phys.*, 1952, 20: 411—424.
- Shao G. and Tsakirooulos P. Prediction of phase selection in rapid solidification using time dependent nucleation theory. *Acta Metall. Mater.*, 1994, 42(9): 2937—2942.
- Tokunaga T., Nishio K., Ohtani H. et al. Thermodynamic assessment of the Ni-Si system by incorporating ab initio energetic calculations into the CALPHAD approach. *Calphad.*, 2003, 27: 161—168.
- Wang N., Han X. J. and Wei B. Specific heat and thermodynamic properties of undercooled liquid cobalt. *Appl. Phys. Lett.*, 2002, 80: 28—30.
- Sung Y. S., Takeya H. and Hirata K. Specific heat capacity and hemispherical total emissivity of liquid Si measured in electrostatic levitation. *Appl. Phys. Lett.*, 2003, 83: 1122—1124.